

1 PULSE – Optogenetic control of gene expression in plants in
2 the presence of ambient white light

3 Rocio Ochoa-Fernandez^{1,2}, Nikolaj B. Abel³, Franz-Georg Wieland⁴, Jenia
4 Schlegel^{2,5}, Leonie A. Koch¹, J. Benjamin Miller⁶, Raphael Engesser⁴, Giovanni
5 Giuriani¹, Simon M. Brandl³, Jens Timmer^{4,7}, Wilfried Weber^{3,7}, Thomas Ott^{3,7},
6 Rüdiger Simon^{2,5,8}, Matias D. Zurbriggen^{1,2,8,#}

7

8 ¹Institute of Synthetic Biology, University of Düsseldorf, Germany

9 ²iGRAD Plant Graduate School, University of Düsseldorf, Germany.

10 ³Faculty of Biology, University of Freiburg, Germany

11 ⁴Institute of Physics, University of Freiburg, Germany

12 ⁵Institute of Developmental Genetics, University of Düsseldorf, Germany

13 ⁶School of Biological Sciences, University of East Anglia, Norwich, UK.

14 ⁷Signalling Research Centres BIOS and CIBSS, University of Freiburg, Germany

15 ⁸CEPLAS - Cluster of Excellence on Plant Sciences, Düsseldorf, Germany

16

17 [#]Corresponding author: MDZ matias.zurbriggen@uni-duesseldorf.de

18 ABSTRACT

19 Optogenetics, the genetic approach of controlling cellular processes with light, is
20 revolutionizing biological signalling and metabolic studies. It provides unmatched
21 spatiotemporal, quantitative and reversible control, overcoming limitations of
22 chemically-inducible systems. However, optogenetics severely lags in plant research
23 because ambient light required for growth leads to undesired system activation. We
24 solved this issue engineering PULSE (Plant Usable Light-Switch Elements), the first
25 optogenetic tool for reversibly controlling gene expression in plants under ambient
26 light. PULSE combines a blue light-regulated repressor with a red light-inducible
27 switch. Gene expression is only activated under red light and remains inactive under
28 white light/darkness. Supported by a quantitative mathematical model we
29 characterized PULSE in protoplasts achieving high induction rates, and combined it
30 with CRISPR/Cas9-based technologies to target synthetic signalling and
31 developmental pathways. We applied PULSE to control immune responses in plant
32 leaves and generated Arabidopsis transgenic plants. PULSE opens broad
33 experimental avenues for plant research and biotechnology.

34

35 INTRODUCTION

36 The reversible and orthogonal control of cellular processes with high spatiotemporal
37 resolution is key for quantitatively understanding the dynamics of biological signalling
38 networks as well as for programming desired phenotypes. The optimal stimulus for
39 such cellular control is light as it can be applied with unmatched spatiotemporal
40 precision in a quantitative manner, with minimized toxicity and invasiveness.

41 Accordingly, optogenetics, the control of cellular events by using genetically
42 encoded, light-responsive switches is opening revolutionary avenues in mammalian
43 systems. A non-limiting list of successfully manipulated and regulated cellular and
44 physiological processes with optogenetic switches includes neuromodulation, gene
45 expression, epigenetics, protein and organellar activity, and subcellular localization¹⁻
46 ⁷.

47 While similar approaches to address important biological questions are needed in
48 plant research, the use of optogenetics to answer them is limited by the intrinsic need
49 of plants for broad-spectrum light which would erroneously activate the engineered
50 light-responsive switches. We have recently developed and successfully
51 implemented the first two optogenetic systems for the control of gene expression in
52 plant cells. The systems are regulated by red and green light and proved useful for
53 the quantitative manipulation of hormone signalling pathways and recombinant
54 protein expression control^{8,9}. However, due to the spectral compatibility limitations
55 described above or the need for co-factors difficult to administer to whole plants,
56 these tools could only be applied in transiently transformed plant cells such as
57 mesophyll protoplasts from *Nicotiana tabacum* or *Arabidopsis thaliana*, and the moss
58 *Physcomitrella patens* which can be kept in the dark prior to the optogenetic
59 experiment⁸⁻¹⁰. Despite their utility for transient signalling studies in cell culture, it is
60 highly desirable to have an optogenetic tool functional in whole plants and being

61 insensitive to broad-spectrum white light to harness the full potential of optogenetics
62 in the plant kingdom.

63 Towards this goal, we set here to develop the first optogenetic system for the control
64 of gene expression in plants that is silent under white light and can be activated with
65 monochromatic red light. The system, termed PULSE (Plant Usable Light-Switch
66 Elements), comprises two engineered photoreceptors exerting a combined activity
67 over the regulation of transcription initiation: one actively represses gene expression
68 under blue light (B_{Off} , Blue Light-repression) engineered from the EL222
69 photoreceptor¹¹, and the second one activates gene expression with red light (R_{On} ,
70 Red Light-activation) based on a Phytochrome B (PhyB) - PIF6 optoswitch^{8,10} (**Fig.**
71 **1**).

72 We first engineered and characterized PULSE in *Arabidopsis thaliana* protoplasts.
73 PULSE provides quantitative and spatiotemporal reversible control over gene
74 expression, achieving high induction rates (up to *ca.* 400-fold) while being Off under
75 white light or in the dark. We developed a mathematical model to quantitatively
76 characterize the dynamic behaviour of the system and guide designing experimental
77 setups. We combined it with a plant transcription factor (TF) or a CRISPR/Cas9-
78 derived gene activator and showed its functionality for the light-controlled activation
79 of both *Arabidopsis* and orthologous promoters. Furthermore, we applied PULSE to
80 engineer light-inducible immunity *in planta* using *Nicotiana benthamiana* leaves as
81 model system, and tested its functionality in whole *Arabidopsis* transgenic plants.
82 These results demonstrate the wide applicability of PULSE, opening up novel
83 perspectives for the targeted spatiotemporal and quantitative study and control of
84 plant signalling, genetic and metabolic networks as well as its implementation for
85 biotechnological approaches.

86

87 RESULTS

88

89 Design, implementation, and test of the PULSE system in plant cells

90 PULSE is an integrated optogenetic molecular device, consisting of two components,
91 a module providing activation of gene expression under red light (R_{On}) and a second
92 one ensuring effective transcriptional repression under blue light (B_{Off}) (**Fig. 1**). The
93 rationale behind this new conceptual and experimental approach is that the
94 combination of both switches will yield a system that is inactive in ambient growth
95 conditions (light and darkness) and only active upon irradiation with red light. This
96 enables full applicability in plants growing under standard light conditions.

97 We first constructed a blue light-regulated gene repression switch B_{Off} based on the
98 photoreceptor EL222 from the bacterium *Erythrobacter litoralis*¹¹ which has a Light-
99 Oxygen-Voltage (LOV) dependent motif and an Helix-Turn-Helix (HTH) domain.
100 Upon blue light it binds as a dimer to the target DNA sequence C120¹². B_{Off} thus
101 comprises (**Fig. 2a**): i) the constitutively expressed EL222 fused to a transcriptional
102 repressor domain (REP), and ii) a reporter module driving the expression of a
103 reporter gene (*e.g.* Firefly luciferase, FLuc) under the control of a synthetic tripartite
104 promoter. The promoter comprises a quintuple-repeat target sequence for EL222,
105 termed (C120)₅, flanked by the enhancer sequence of the CaMV35S promoter and
106 the minimal domain of the constitutive promoter hCMV.

107 We evaluated three versions of the blue light-repressor module by fusing either of
108 three different known transrepressor domains to the N-terminus of EL222, one from
109 the human Krüppel Associated Box (KRAB)^{13,14} protein, and two from Arabidopsis,
110 namely the B3 repression domain (BRD)¹⁵ and the EAR repression domain (SRDX)¹⁵
111 (**Fig. 2a**). The functionality of the B_{Off} optoswitches was assayed by transient co-
112 transformation with the reporter construct into Arabidopsis protoplasts. Constitutively

113 expressed Renilla luciferase, RLuc, was included for normalization. The cells were
114 illuminated for 18 h at different light intensities of blue light (0, 0.25, 0.5, 1, 5 and 10
115 $\mu\text{mol m}^{-2} \text{s}^{-1}$), and FLuc/RLuc activity was quantified (**Fig. 2b**). These blue light
116 intensities had no negative effect on protoplast performance. All three versions of the
117 repressor modules were functional although with different efficiencies, yielding a
118 range of repression levels (SRDX, 92%; BRD, 84%; and KRAB, 53%; at 10 $\mu\text{mol m}^{-2}$
119 s^{-1} blue light). Based on the highest repression level and dynamic range achieved,
120 we decided to use SRDX-EL222 as a trans-repressor module for all subsequent
121 experiments.

122 To allow gene induction with PULSE, we then combined the novel blue light-
123 repressible (B_{Off}) module with our previously developed PhyB – PIF6 red light-
124 inducible split TF switch (R_{On})^{8,10} (**Fig. 3a,b**). PULSE thus integrates: i) a
125 constitutively expressed red light-activation module composed of PhyB-VP16 and E-
126 PIF6, ii) a constitutively expressed blue light-repressor module SRDX-EL222, and iii)
127 a synthetic target promoter, P_{Opto} , integrating the binding domains for both switches,
128 namely $(C120)_5$ and $(\text{etr})_8$, upstream of a hCMV minimal promoter sequence driving
129 the expression of a gene of interest. In the presence of blue or white light (a
130 combination of blue, green, red and far-red wavelengths as present in ambient light)
131 both photoreceptors PhyB and EL222 bind to P_{Opto} . The net result of the recruitment
132 of the transcriptional activator and repressor near to the minimal promoter sets the
133 system to the Off state. This also applies to darkness and far red light conditions, as
134 the red light-switch is rendered inactive under these wavelengths. Under any other
135 illumination condition lacking the blue light component, SRDX-EL222 is unable to
136 bind P_{Opto} and thus to repress transcription. The system is, then, exclusively in the
137 On state upon monochromatic red light treatment when the interaction between PhyB

138 and PIF6 leads to the recruitment of the activation domain to the minimal promoter
139 inducing gene expression (**Fig. 3a**).

140 The PULSE system controlling FLuc expression was first introduced and tested in
141 isolated Arabidopsis protoplasts (**Fig. 3c**). The plasmids coding for the R_{on} switch
142 were co-transformed either with or without B_{off} , and the protoplasts were incubated
143 for 18 h under either red, blue, white or far-red light (as described in **Methods**). In the
144 absence of the repressor module (equivalent to R_{on}), efficient activation of PhyB was
145 observed by red light but also under blue and white, as UV and blue light (300 - 460
146 nm) also activate PhyB^{16,17}. Upon addition of the B_{off} repressor module (PULSE
147 system) we observed induction under red light treatment only, showing a high
148 dynamic range, with up to 396.5-fold induction rates relative to darkness, and a very
149 low basal level of expression in blue and white light (1.7- and 1.6-fold, respectively).

150

151 **Development and application of a quantitative model to describe and predict** 152 **the PULSE activity**

153 In order to quantitatively understand the dynamics and functional characteristics of
154 PULSE and to guide the experimental design of future applications concerning
155 optimal light quality, intensity, and duration, we developed an ordinary differential
156 equation (ODE)-based quantitative mathematical model. The **Supplementary**
157 **Information** provides a detailed derivation of the model equations, error
158 measurements, system parameters and uncertainty analysis performed. To
159 parameterize the model, On-Off kinetic studies of the PULSE system were performed
160 in protoplasts by monitoring FLuc protein and mRNA levels (**Extended Data Fig.**
161 **1a,b**). The experiments demonstrate the reversibility of the system. In order to further
162 characterize thresholds of time and light intensity for protein production, end point
163 measurements and dose-response experiments were performed (**Supplementary**

164 **Fig. 1a,b,c).** Next, we used the parameterized model to predict the experimental
165 gene expression outcomes of the system as a function of different light intensities,
166 wavelengths and illumination times. Heat maps were generated based on simulations
167 of the dynamic behaviour of PULSE (**Extended Data Fig. 1c, Supplementary Fig.**
168 **2)** which will aid in the experimental design by guiding the targeted selection of
169 conditions to obtain a given expression level of interest. To illustrate this, PULSE was
170 tested for combinations of red light intensities and illumination durations selected
171 from the heatmap. A strong correspondence between predicted and experimentally
172 determined activities was observed (**Extended Data Fig. 1c,d**). This indicates the
173 applicability of the model to determine the experimental conditions needed to achieve
174 a tight control over the levels of gene expression with PULSE.

175

176 **PULSE-controlled expression of CRISPR/Cas9-derived gene activator and plant** 177 **TFs to regulate orthologous and plant promoters in Arabidopsis protoplasts**

178 We next set out to customize PULSE to achieve quantitative and temporally resolved
179 control over the expression of genes from any given promoter of interest, be it
180 orthologous, synthetic or endogenous (downstream activation). For this we devised
181 two approaches applying PULSE: i) to induce the synthesis of a CRISPR/Cas9-
182 derived gene activator, or ii) to induce expression of an endogenous TF. These
183 expressed transcriptional activators, in turn, activate expression from target
184 orthologous (**Fig. 4a,b**) or Arabidopsis promoters (**Fig. 4c-f**).

185 To achieve optogenetic and customizable control of potentially any target promoter,
186 PULSE was set to control expression of a nuclease-deficient *Streptococcus*
187 *pyogenes* Cas9 protein fused to a strong activation domain (termed dCas9TV)^{18,19}. In
188 a first proof of principle application, PULSE-induced dCas9-TV was used to drive
189 expression from an orthologous promoter, the *Solanum lycopersicum* dihydroflavonol

190 4-reductase promoter (P_{SIDFR}), using FLuc as a quantitative readout in Arabidopsis
191 protoplasts (**Fig. 4a**). To target the promoter, a gRNA against the -150 bp region
192 relative to the transcription start site (TSS) of P_{SIDFR} was used¹⁹. PULSE-controlled
193 dCas9-TV led to activation of the promoter only upon red illumination, achieving 24.5-
194 and 40.0-fold induction rate compared to blue light and dark treatments, respectively
195 (**Fig. 4b**). Constitutive expression of dCas9-TV served as a positive control yielding
196 the maximum activation capacity of P_{SIDFR} , 105.1-fold induction relative to the
197 configuration without dCas9-TV (**Supplementary Fig. 3a**). In a second set up,
198 optogenetically-induced dCas9-TV targeted the promoter of the Arabidopsis gene
199 APETALA1 (P_{AtAP1}) which includes the 5'UTR and 2,781 bp upstream of the TSS
200 fused to the reporter FLuc (P_{AtAP1} -FLuc) in a plasmid. A gRNA was designed to target
201 the -100 bp region relative to the TSS of P_{AtAP1} (**Fig. 4c**). Red light induction of
202 dCas9-TV yielded 17.9- and 14.1-fold FLuc induction rates from the P_{AtAP1} -FLuc
203 construct compared to blue and dark illumination (**Fig. 4e**). Constitutive expression of
204 dCas9-TV yielded a 28.6-fold induction relative to the configuration without dCas9-TV
205 (**Supplementary Fig. 3b**).

206 We next configured PULSE to drive the expression of the Arabidopsis TF LEAFY
207 (LFY) that is known to bind P_{AtAP1} and promote the expression of AP1²⁰. LFY and
208 AP1 are involved in Arabidopsis flowering and both are expressed in the floral
209 primordia. LFY was fused to the transactivator VP16 and RLuc using a self-cleaving
210 2A sequence, which yields equimolar amounts of both proteins from a single
211 transcript²¹ (P_{Opto} -LFY-VP16-2A-RLuc). RLuc allows the indirect quantification of the
212 amount of LFY protein synthesized (**Fig. 4d**). The PULSE plasmids were co-
213 transformed in Arabidopsis protoplasts either with or without the optogenetically
214 inducible LFY, and a P_{AtAP1} -FLuc target plasmid. RLuc values indicate expression of
215 LFY-VP16 upon red light treatment, while only basal levels were obtained upon blue

216 light or dark treatment (17.5- and 26.6-fold induction, respectively). The red light-
217 induced expression of LFY-VP16 led to activation of P_{AtAP1} and, therefore, FLuc
218 expression achieving 31.4- and 7.4-fold induction rates compared to blue and
219 darkness conditions, respectively (**Fig. 4f**, controls in **Supplementary Fig. 3c**).

220

221 ***In planta* optogenetic control of gene expression with PULSE**

222 We next set to evaluate the functionality of PULSE in plants. For this, a new set of
223 vectors was engineered for transformation via *Agrobacterium tumefaciens* with all
224 necessary components in binary plasmids. The vectors comprise a reporter gene
225 under the control of PULSE (P_{Opto}), PULSE expressed under a constitutive promoter
226 (either $P_{CaMV35S}$ or $P_{AtUbi10}$), and optionally, a constitutively expressed reporter gene
227 as a normalization element and a plant selection cassette (full description of vectors
228 in **Supplementary Table 1**).

229 *N. benthamiana* leaves were transiently transformed with a construct having PULSE,
230 a fluorescent protein gene as a reporter (Venus fused to histone H2B for nuclear
231 localization, P_{Opto} -Venus-H2B) and constitutively expressed Cerulean fused to a
232 nuclear localization sequence (NLS) as a normalization element. The plants showed
233 an increase in nuclear Venus/Cerulean fluorescence ratio over time when treated
234 with red light, reaching 28.7-fold induction after 9 h and keeping background levels in
235 blue, dark and white light, demonstrating activation of the system *in planta* (**Fig. 5a,b**
236 and **Supplementary Fig. 4**). Additionally, PULSE control over a β -glucuronidase
237 gene (P_{Opto} -GUS) is shown in **Supplementary Fig. 5**.

238

239 ***In planta* optogenetic induction of immunity and conditional subcellular** 240 **fluorescent targeting of receptors**

241 In plants, signal integration of extracellular stimuli is predominantly mediated by
242 membrane-resident receptor and transport complexes. To mechanistically
243 understand their function, we require non-invasive inducible systems that allow
244 transcriptional induction or complex formation with high temporal precision in order to
245 reconstitute these functional entities in homologous as well as heterologous systems.
246 To test this, we asked whether PULSE allows the generation of immune-competent
247 leaf epidermal cells by introducing a heterologous pattern recognition receptor.
248 In *Arabidopsis*, the recognition of the bacterial microbe-associated molecular pattern
249 (MAMP) elf18 by the plant innate immune EF-Tu Receptor (EFR) results in a fast and
250 transient increase in cellular reactive oxygen species (ROS)²². By contrast,
251 Solanaceae species such as *N. benthamiana* are devoid of EFR and therefore
252 unable to perceive the elf18 peptide. However, genetic transformation of *N.*
253 *benthamiana* and *S. lycopersicum* with *AtEFR* allows these plants to recognize elf18
254 and confers increased resistance against phytopathogens such as *Ralstonia*
255 *solanacearum*^{22,23}. To achieve optogenetically controlled induction of immunity we
256 expressed an EFR-GFP fusion protein under the control of PULSE (P_{Opto}-EFR-GFP)
257 in *N. benthamiana* leaf epidermal cells (**Fig. 6a**). Red light treatment of leaves for 16
258 h resulted in a clear GFP signal at the cell periphery indicating that EFR-GFP was
259 successfully localized to the plasma membrane (**Supplementary Fig. 6**). To test
260 whether optogenetically controlled EFR provides susceptibility of these cells towards
261 elf18, we applied 1 μ M of the elf18 ligand. Indeed, a strong and transient production
262 of ROS was observed *ca.* 10 min after elf18 application in leaves that have been red
263 light-treated (red filled circles; **Fig. 6b**). Quantitative assays showed around 10-fold
264 lower ROS burst triggered in white light-grown plants (black filled circles; **Fig. 6b**),
265 demonstrating light-repression by PULSE under ambient light conditions. No
266 responses were found in untransformed tissue and leaves expressing EFR, but

267 incubated in the absence of elf18. It should be noted that MAMP-triggered ROS
268 production also relies on a self-amplifying mechanism. ROS spread to neighbouring
269 cells where they induce calcium fluxes leading to the activation of the ROS-producing
270 protein respiratory burst oxidase homolog protein D (RBOHD)^{24,25}. Thus, ROS will be
271 detected even at very low background levels of EFR in this system. These data show
272 that PULSE can be used for inducing physiological responses *in planta* in a time-
273 controlled manner.

274 Next, we set to test the applicability of PULSE for conditional targeting of receptors
275 using nanobodies. In mammalian cells, receptor complexes have been reconstituted
276 and modulated using genetically encoded nanobodies^{26,27}. Given their small size and
277 their high-affinity binding characteristics, nanobodies can be used to subcellularly
278 relocalize proteins in a stimulus-dependent manner or to visualize endogenous
279 proteins (using fluorophore-tagged nanobodies). We constitutively expressed the
280 immune receptor EFR-GFP in *N. benthamiana* leaf epidermal cells and co-
281 transformed a genetically encoded GFP nanobody (GFP binding protein, GBP) that
282 binds GFP²⁸. To monitor localization, we additionally fused GBP to mCherry and
283 placed it under the control of PULSE (P_{Opto}-GBP-mCherry). (**Fig. 6c**). Red light-
284 induction of GBP-mCherry expression in EFR-deficient cells resulted in a cytosolic
285 localization of the soluble protein. By contrast, red light-induction in cells
286 constitutively expressing EFR-GFP showed an almost exclusive targeting of the
287 fluorescently-tagged nanobody to the plasma membrane (**Fig. 6d**). This illustrates
288 potential applications using PULSE-driven genetically encoded specific nanobodies
289 to conduct time-resolved conditional precision targeting of plasma membrane-
290 localized proteins, e.g. targeting proteins for degradation or inhibition similarly to what
291 has been described in animal cells^{26,27,29}. This approach could thus provide novel
292 opportunities to non-invasively control signalling processes in plants.

293

294 **PULSE functionality in stable Arabidopsis transgenic lines**

295 To test the functionality of PULSE in whole plants, transgenic Arabidopsis lines were
296 generated using the plasmid coding for PULSE under the control of the $P_{CaMV35S}$
297 promoter and P_{Opto} -FLuc as a reporter (BM00654). Seedlings of homozygous T3
298 plants were grown in a multi-well plate for 7 days, before incubation with luciferin.
299 The luminescence was quantified while the plate was subjected to different light
300 treatments as indicated in **Fig. 6e**. The results for two independent PULSE lines, #4-
301 4 and #6-3, show that the system is functional with activation levels ranging from 10-
302 to 21-fold, respectively (determined after 12 h of red light, t_{36h} , compared to right
303 before the induction, t_{24h}). Transfer from white light to red light led to activation of
304 expression, and subsequent inactivation was achieved when the plants were moved
305 back to white light (**Fig. 6e**), demonstrating reversibility of the system, which was
306 verified also in a second cycle. This is the first example of an optogenetic tool
307 controlling gene expression in whole plants, opening up unforeseen opportunities for
308 plant research and biotechnology.

309

310 **DISCUSSION**

311 In order to study and understand cellular processes, it is required to be able to
312 achieve a precise spatiotemporal and quantitative control over their regulation.
313 Genetically encoded chemical-inducible systems have been widely employed for the
314 targeted manipulation of gene expression and other signalling events in prokaryotic
315 and diverse eukaryotic organisms, including plants³⁰⁻³². However, they suffer from
316 intrinsic drawbacks including limited temporal and spatial resolution, diffusion effects,
317 and constrains to deactivate the system after the application of the inducer, in
318 addition to potential pleiotropic activity and toxicity. Some of these experimental

319 constraints can be solved by using light as an inducer. A plant's requirement for light
320 to grow, however, limits the implementation of optogenetic approaches, as ambient
321 light leads to undesired activation of most currently available light-controlled systems.
322 Consequently, most of the advantages of optogenetics which have been recently
323 revolutionizing animal and microbial research are simply not applicable in plants. A
324 recent optogenetic approach challenged a plant intrinsic physiological conundrum,
325 namely, how to conserve water under hydric stress by minimizing transpiration
326 without limiting CO₂ uptake, two processes directly regulated by stomatal aperture.
327 Papanatsiou *et al.*³³ resorted to a synthetic, blue light-gated K⁺ channel (BLINK1),
328 engineered for the control of K⁺ conductance in animal cells³⁴. Guard cell-specific
329 expression of BLINK1 in Arabidopsis led to accelerated kinetics of ion fluxes (full
330 activation after 2 min blue light), with reduction of mean stomatal opening and
331 closure half-life times by 40-70% in comparison to wild type controls. Faster stomatal
332 movements improved gas exchange efficiency under fluctuating light conditions,
333 resulting in a more efficient water use without a trade-off in carbon assimilation. This
334 tool profits from the fact that it is applied to a process that is photosynthesis-
335 dependent therefore occurring already naturally under ambient light.
336 Towards a more generalized application of optogenetic in plants, creative
337 engineering approaches are needed. We set here to design an optogenetic device
338 for the control of gene expression in plants that overcomes the intrinsic challenges,
339 namely, that is non-responsive to ambient illumination conditions and can be only
340 activated by illuminating with a specific, narrow wavelength spectrum. The novel
341 concept implements the design of a dual-wavelength optogenetic switch combining a
342 blue light-regulated repressor with a red light-inducible gene expression switch.
343 PULSE introduces the superior experimental assets of optogenetic systems into
344 plants. The system showed a high dynamic range in Arabidopsis protoplasts with *ca.*

345 400-fold (red light vs. darkness) induction, reversibility and no toxicity. PULSE is
346 applicable for the targeted study of signalling and metabolic networks by, in principle,
347 allowing the control of any endogenous or synthetic promoter of interest as
348 exemplified with the light-driven expression of a plant TF or of a CRISPR/Cas9-
349 derived transcriptional activator. *In planta*, implementation of PULSE demonstrated
350 tight temporal control over subcellular conditional protein targeting, and the capability
351 to induce immunity in *N. benthamiana* leaves. The system is functional in Arabidopsis
352 plants, showing high dynamic range of transgene expression when activated with red
353 light and reversibility when the plants were returned to white light. PULSE could in
354 the future be combined with tissue-specific promoters for organ or developmentally
355 specific expression and activity, as currently done for genetically encoded biosensors
356 and other tools. When using different promoters, the dynamic range of induction
357 might be affected, therefore usage-specific optimizations might be necessary.

358 By using only the N-terminus of PhyB (amino acids 1-650) and the first 100 amino
359 acids of PIF6, we intend to minimize potential interactions of the system with
360 endogenous plant components (EL222 is of bacterial origin, therefore we do not
361 expect any considerable effect on plant signalling). However, we cannot rule out a
362 possible PULSE cross-talk with the endogenous signalling (PhyB) pathway. This is
363 an unavoidable cost to pay in exchange of getting a new functionality as it is also the
364 case when using chemically inducible switches^{30,31} or genetically encoded
365 biosensors, e.g. some hormone sensors can lead to hormone hypersensitivity
366 phenotypes, as previously exemplified and discussed³⁵.

367 The strategy here presented, based on engineering and combining switches
368 sensitive to different wavelengths, can be expanded to inspire the engineering of
369 other optogenetic tools compatible with the plant's growth needs. These will likely not
370 be restricted to transcriptional regulation but could also be extended to the

371 application of selected mammalian optogenetic systems with a high transfer interest
372 to the plant community, *e.g.* to control cellular receptors, kinase activity, ion and
373 metabolite transporters, among other cellular processes^{1,36}. For example, signalling
374 proteins could be engineered for red light-regulated recruitment to sub-cellular
375 locations where they activate a signalling cascade, *e.g.* to the plasma membrane as
376 described in mammalian cells^{37,38}. To prevent activation under white light, the same
377 signalling protein could additionally be targeted for degradation under blue light by
378 fusing it to a blue light-inducible degron^{14,39,40}. Alternatively it could be sequestered to
379 the nucleus under white light by fusing it to the blue light-responsive LINuS⁴¹ or
380 LANS systems⁴². Hence, only under exclusive red light treatment, the protein would
381 be targeted to the site of activity in the cytoplasm or plasma membrane and exert its
382 function.

383 In this work, we pioneer the optogenetic control of gene expression in plants under
384 ambient light, reflecting the ground-breaking opportunities for plant fundamental and
385 biotechnological fields provided by optogenetics. Due to the quantitative modulation,
386 spatiotemporal resolution and the reversible control capabilities provided, we think
387 that a generalized application of PULSE will facilitate the targeted manipulation and
388 study of biological processes including development, metabolism, hormone
389 signalling, and stress responses.

390 **ACKNOWLEDGEMENTS**

391 This study was in part supported by the Deutsche Forschungsgemeinschaft (DFG,
392 German Research Foundation) under Germany's Excellence Strategy (CEPLAS –
393 EXC-1028 Project ID 194465578 to RS and MDZ, EXC-2048/1 – Project ID
394 390686111 to RS and MDZ, CIBSS – EXC-2189 – Project ID 390939984 to T.O.,
395 J.T. and W.W., and BIOS – EXC-294 to J.T., T.O. and W.W.), the iGRAD Plant
396 (IRTG 1525 to R.O., J.S., R.S., M.D.Z.), and the Collaborative Research Centers
397 SFB1208 (Project-ID 267205415; project A13 to M.D.Z.) and SFB924 (INST
398 95/1126-2; project B4 to T.O.), the European Commission – Research Executive
399 Agency (H2020 Future and Emerging Technologies FET-Open Project ID 801041
400 CyGenTig to M.D.Z.). J.B.M. is supported by a fellowship from the Eastern Academic
401 Research Consortium. We thank D. Orzaez for kindly providing the GoldenBraid
402 plasmids, T. Brumbarova for aid on RT-qPCR experiments, R. Wurm and M. Gerads
403 for technical assistance, and J. Schmidt for designing and constructing the light
404 boxes used in this work. We are indebted to J. Casal, D. Nusinow, S. Romero, H.
405 Beyer and U. Urquiza for careful reading and suggestions to improve the manuscript.

406 **AUTHOR CONTRIBUTIONS**

407 R.O., N.B.A., L.A.K., B.M., and S.B. designed and cloned the constructs. S.B.
408 performed preliminary tests and R.O.F. conducted all Arabidopsis protoplasts
409 experiments. F.W. and R.E. developed the mathematical model. R.O., N.B.A., J.S.,
410 and L.A.K. contributed to the establishment of PULSE *in planta*. N.B.A. conducted
411 the conditional targeting and immunity induction *in planta*. R.O.F. and G.G.
412 generated the transgenic Arabidopsis PULSE lines and performed the experiments.
413 R.O., N.B.A., T.O., R.S., and M.D.Z. designed the experiments. J.T., W.W., T.O.,
414 R.S., M.D.Z. supervised the research. T.O., R.S., and M.D.Z. analyzed the data and

415 discussed results. M.D.Z. planned and directed the project. R.O. and M.D.Z.
416 designed the system and wrote the initial manuscript with input from all authors. All
417 authors contributed to editing and read the final version of the manuscript.

418 ETHICS DECLARATION

419 The authors declare no competing interests.

420

421 REFERENCES (main text)

- 422 1. Deisseroth, K. & Hegemann, P. The form and function of channelrhodopsin.
423 Science 357, eaan5544 (2017).
- 424 2. Alberio, L. et al. A light-gated potassium channel for sustained neuronal inhibition.
425 Nat. Methods 15, 969–976 (2018).
- 426 3. Ye, H., Baba, M. D.-E., Peng, R.-W. & Fussenegger, M. A Synthetic Optogenetic
427 Transcription Device Enhances Blood-Glucose Homeostasis in Mice. Science
428 332, 1565 (2011).
- 429 4. Strickland, D. et al. TULIPs: tunable, light-controlled interacting protein tags for cell
430 biology. Nat. Methods 9, 379–84 (2012).
- 431 5. Shin, Y. et al. Spatiotemporal Control of Intracellular Phase Transitions Using
432 Light-Activated optoDroplets. Cell 168, 159-171.e14 (2017).
- 433 6. van Bergeijk, P., Adrian, M., Hoogenraad, C. C. & Kapitein, L. C. Optogenetic
434 control of organelle transport and positioning. Nature 518, 111–4 (2015).
- 435 7. Kolar, K., Knobloch, C., Stork, H., Žnidarič, M. & Weber, W. OptoBase: A Web
436 Platform for Molecular Optogenetics. ACS Synth. Biol. 7, 1825–1828 (2018).
- 437 8. Müller, K. et al. A red light-controlled synthetic gene expression switch for plant
438 systems. Mol Biosyst 10, 1679–88 (2014).
- 439 9. Chatelle, C. et al. A Green-Light-Responsive System for the Control of Transgene
440 Expression in Mammalian and Plant Cells. ACS Synth. Biol. 7, 1349–1358
441 (2018).
- 442 10. Ochoa-Fernandez, R. et al. Optogenetics: Methods and Protocols. in (ed.
443 Kianianmomeni, A.) 125–139 (Springer New York, 2016). doi:10.1007/978-1-
444 4939-3512-3_9.

- 445 11. Nash, A. I. et al. Structural basis of photosensitivity in a bacterial light-oxygen-
446 voltage/helix-turn-helix (LOV-HTH) DNA-binding protein. *Comput. Biol.* 108,
447 9449–945 (2011).
- 448 12. Motta-Mena, L. B. et al. An optogenetic gene expression system with rapid
449 activation and deactivation kinetics. *Nat. Chem. Biol.* 10, 196–202 (2014).
- 450 13. Moosmann, P., Georgiev, O., Thiesen, H., Hagmann, M. & Schaffner, W.
451 Silencing of RNA polymerases II and III-dependent transcription by the KRAB
452 protein domain of KOX1, a Krüppel-type zinc finger factor. *Biol. Chem.* 378, 669–
453 677 (1997).
- 454 14. Baaske, J. et al. Dual-controlled optogenetic system for the rapid down-regulation
455 of protein levels in mammalian cells. *Sci. Rep.* 8, 15024 (2018).
- 456 15. Ikeda, M. & Ohme-Takagi, M. A novel group of transcriptional repressors in
457 *Arabidopsis*. *Plant Cell Physiol.* 50, 970–975 (2009).
- 458 16. Kelly, J. M. & Lagarias, J. C. Photochemistry of 124-kilodalton *Avena*
459 phytochrome under constant illumination in vitro. *Biochemistry* 24, 6003–6010
460 (1985).
- 461 17. Müller, K. et al. Multi-chromatic control of mammalian gene expression and
462 signaling. *Nucleic Acids Res.* 41, e124 (2013).
- 463 18. Li, Z. et al. A potent Cas9-derived gene activator for plant and mammalian cells.
464 *Nat. Plants* 3, 930–936 (2017).
- 465 19. Selma, S. et al. Strong gene activation with genome-wide specificity using a new
466 orthogonal CRISPR/Cas9-based Programmable Transcriptional Activator. *bioRxiv*
467 486068 (2018) doi:10.1101/486068.
- 468 20. Simon, R., Igeño, M. I. & Coupland, G. Activation of floral meristem identity genes
469 in *Arabidopsis*. *Nature* 384, 59–62 (1996).

- 470 21. de Felipe, P. et al. E unum pluribus: multiple proteins from a self-processing
471 polyprotein. *Trends Biotechnol.* 24, 68–75 (2006).
- 472 22. Zipfel, C. et al. Perception of the Bacterial PAMP EF-Tu by the Receptor EFR
473 Restricts *Agrobacterium*-Mediated Transformation. *Cell* 125, 749–760 (2006).
- 474 23. Lacombe, S. et al. Interfamily transfer of a plant pattern-recognition receptor
475 confers broad-spectrum bacterial resistance. *Nat. Biotechnol.* 28, 365 (2010).
- 476 24. Suzuki, N. et al. Respiratory burst oxidases: the engines of ROS signaling. *Curr.*
477 *Opin. Plant Biol.* 14, 691–699 (2011).
- 478 25. Gaupels, F., Durner, J. & Kogel, K.-H. Production, amplification and systemic
479 propagation of redox messengers in plants? The phloem can do it all! *New*
480 *Phytol.* 214, 554–560 (2017).
- 481 26. Kirchhofer, A. et al. Modulation of protein properties in living cells using
482 nanobodies. *Nat. Struct. Mol. Biol.* 17, 133 (2009).
- 483 27. Gulati, S. et al. Targeting G protein-coupled receptor signaling at the G protein
484 level with a selective nanobody inhibitor. *Nat. Commun.* 9, 1996 (2018).
- 485 28. Schornack, S. et al. Protein mislocalization in plant cells using a GFP-binding
486 chromobody. *Plant J.* 60, 744–754 (2009).
- 487 29. Yu, D. et al. Optogenetic activation of intracellular antibodies for direct modulation
488 of endogenous proteins. *Nat. Methods* 16, 1095–1100 (2019).
- 489 30. Moore, I., Samalova, M., Kurup, S., For, T. & Analysis, M. Transactivated and
490 chemically inducible gene expression in plants. *Plant J.* 45, 651–683 (2006).
- 491 31. Zuo, J. & Chua, N. H. Chemical-inducible systems for regulated expression of
492 plant genes. *Curr. Opin. Biotechnol.* 11, 146–151 (2000).
- 493 32. Andres, J., Blomeier, T. & Zurbriggen, M. D. Synthetic Switches and Regulatory
494 Circuits in Plants. *Plant Physiol.* 179, 862–884 (2019).

- 495 33. Papanatsiou, M. et al. Optogenetic manipulation of stomatal kinetics improves
496 carbon assimilation, water use, and growth. *Science* 363, 1456–1459 (2019).
- 497 34. Cosentino, C. et al. Engineering of a light-gated potassium channel. *Science* 348,
498 707–710 (2015).
- 499 35. Martin-Arevalillo, R. & Vernoux, T. Shining light on plant hormones with
500 genetically encoded biosensors. *Biol. Chem.* 400, 477–486 (2018).
- 501 36. Kolar, K. & Weber, W. Synthetic biological approaches to optogenetically control
502 cell signaling. *Curr. Opin. Biotechnol.* 47, 112–119 (2017).
- 503 37. Levskaya, A., Weiner, O. D., Lim, W. A. & Voigt, C. A. Spatiotemporal control of
504 cell signalling using a light-switchable protein interaction. *Nature* 461, 997–1001
505 (2009).
- 506 38. Toettcher, J. E., Weiner, O. D. & Lim, W. A. Using optogenetics to interrogate the
507 dynamic control of signal transmission by the Ras/Erk module. *Cell* 155, 1422–
508 1434 (2013).
- 509 39. Renicke, C., Schuster, D., Usherenko, S., Essen, L. O. & Taxis, C. A LOV2
510 domain-based optogenetic tool to control protein degradation and cellular
511 function. *Chem. Biol.* 20, 619–626 (2013).
- 512 40. Bonger, K. M., Rakhit, R., Payumo, A. Y., Chen, J. K. & Wandless, T. J. General
513 method for regulating protein stability with light. *ACS Chem. Biol.* 9, 111–115
514 (2014).
- 515 41. Niopek, D. et al. Engineering light-inducible nuclear localization signals for
516 precise spatiotemporal control of protein dynamics in living cells. *Nat. Commun.*
517 5, 4404 (2014).
- 518 42. Yumerefendi, H. et al. Control of Protein Activity and Cell Fate Specification via
519 Light-Mediated Nuclear Translocation. *PLoS ONE* 10, e0128443 (2015).

520 **FIGURE LEGENDS**

521 **Fig. 1.** Design of PULSE, a functional optogenetic system for the control of gene
522 expression in plants grown under standard light/dark cycles. Plants require light to
523 grow and this poses an experimental challenge to the implementation of optogenetic
524 switches in plants as they will be activated under ambient conditions. To avoid this
525 issue, we designed PULSE (Plant Usable Light Switch-Element), an optogenetic tool
526 that combines a blue light-regulated repressor (B_{Off}) with a red light-inducible gene-
527 expression switch (R_{On}). In this way gene expression is active only upon illumination
528 with monochromatic red light, while remaining inactive in darkness and under blue,
529 far-red, and white light, hence being applicable to plants grown under standard
530 day/night cycles. (+), presence; (-), absence.

531 **Fig. 2:** Design and characterization of the blue light-regulated gene repression switch
532 (B_{Off}) in Arabidopsis protoplasts. **(a)** Constructs and mode of function. The
533 components engineered and characterized in plant cells are: i) the blue light-
534 responsive *E. litoralis* photoreceptor EL222 fused to either of three different repressor
535 (REP-EL222) domains: KRAB, BRD, SRDX and placed under the control of the
536 constitutive promoter P_{CaMV35S} , ii) a synthetic promoter composed of the enhancer
537 region of P_{CaMV35S} , five repeats of C120 - (C120)₅ - and a minimal promoter P_{hCMV} ,
538 driving the expression of the reporter gene FLuc, and iii) P_{CaMV35S} driving the
539 constitutive expression of the normalization element RLuc. The transcription factor
540 EL222 has a Light-Oxygen-Voltage (LOV) dependent domain and a Helix-Turn-Helix
541 (HTH) domain. The photoreceptor is folded in the dark due to a flavin-protein adduct
542 and incapable of binding to the (C120)₅ element. As a result, expression of FLuc is
543 constitutively active. Upon blue light illumination REP-EL222 unfolds allowing the
544 formation of dimers binding to the (C120)₅ element via the HTH. As a result, the
545 initiation of FLuc transcription is repressed. **(b)** Characterization of the system.
546 Arabidopsis protoplasts were transformed with the reporter module (pROF402) and
547 the blue light-responsive element (photoreceptor, EL222) fused to either repressor:
548 KRAB (pROF018), BRD (pROF050), and SRDX (pROF051) or without the
549 optoswitch (\emptyset , stuffer plasmid). Constitutively expressed RLuc (GB0109) was
550 included for normalization. After transformation, protoplasts were kept in darkness or
551 illuminated with different intensities of blue light (0.25, 0.5, 1, 5, 10 $\mu\text{mol m}^{-2} \text{s}^{-1}$), and
552 FLuc and RLuc were determined after 18 h. Shown data are FLuc/RLuc ratios of
553 distinct protoplasts samples ($n = 6$), bars are the mean ratios and error bars indicate
554 standard error of the mean (SEM). RLU = Relative Luminescence Units. NLS =
555 Nuclear Localization Sequence.

556 **Fig. 3:** Molecular design and functional characterization of PULSE in Arabidopsis
557 protoplasts. **(a,b)** Mode of function of PULSE and constructs engineered: i) blue light-
558 photoreceptor EL222 fused to the SRDX repressor domain (B_{Off}), ii) red light-
559 activated/far-red light-inactivated (reversible) split switch comprising the first 650
560 amino acids of the PhyB photoreceptor (PhyB_{1-650}) fused to the VP16 transactivation
561 domain, and the DNA-binding protein E 8mphR(A) fused to the first 100 amino acids
562 of PIF6 (PIF_{1-100})⁸ (R_{On}). The B_{Off} and R_{On} modules are constitutively expressed
563 (promoter P_{CaMV35S}), iii) synthetic promoter P_{Opto} comprising target sequence of the
564 protein E, $(\text{etr})_8$, $(\text{C120})_5$, and the minimal promoter P_{hCMVmin} , driving expression of
565 the reporter FLuc, iv) normalization element RLuc expressed constitutively
566 (P_{CaMV35S}). Under white/ambient or blue light, SRDX-EL222 binds to $(\text{C120})_5$, and
567 PhyB is also active (PhyB_{ir}) due to the blue and red light components of white
568 light^{16,17}, and therefore interacts with PIF6, which is bound to $(\text{etr})_8$ through the E
569 protein. In consequence both VP16 and SRDX are recruited to the minimal promoter,
570 resulting in no expression of FLuc as the repressor has a dominant effect on gene
571 expression (left). In darkness or in far-red light EL222 and PhyB are inactive (PhyB_{r}),
572 therefore not binding to P_{Opto} , resulting in no FLuc transcription (middle). There is
573 FLuc expression only under monochromatic red light, in which EL222 is inactive and
574 PhyB is active (right). **(c)** Functional characterization of PULSE. Arabidopsis
575 protoplasts were transformed with the normalization element, reporter P_{Opto} -FLuc,
576 R_{On} module and either with the B_{Off} module (PULSE system complete) or without B_{Off}
577 (stuffer plasmid, equivalent to the R_{On} system alone). Protoplasts were kept in the
578 dark or illuminated with white LEDs, or $10 \mu\text{mol m}^{-2} \text{s}^{-1}$ of $\text{red}_{\lambda_{\text{max}} 655\text{nm}}$, $\text{blue}_{\lambda_{\text{max}} 461\text{nm}}$,
579 or $\text{far-red}_{\lambda_{\text{max}} 740\text{nm}}$ light. FLuc/RLuc ratios of distinct protoplast samples ($n = 6$)
580 determined 18 h after illumination, mean and SEM are plotted. RLU = Relative
581 Luminescence Units. NLS = Nuclear Localization Sequence.

582 **Fig. 4:** PULSE-controlled expression of a Cas9-derived gene activator (dCas9-TV)
583 and an Arabidopsis transcription factor (LFY) in Arabidopsis protoplasts. **(a,b)**
584 PULSE drives dCas9-TV expression ($P_{\text{Opto-dCas9-TV}}$) under red light. dCas9-TV
585 targets the orthologous P_{SIDFR} promoter activating FLuc expression in Arabidopsis
586 protoplasts. **(c-f)** Optogenetic control of an Arabidopsis promoter from a plasmid
587 construct ($P_{\text{AtAP1-FLuc}}$) via two approaches: i) PULSE drives dCas9-TV expression
588 ($P_{\text{Opto-dCas9-TV}}$). dCas9-TV activates expression from $P_{\text{AtAP1-FLuc}}$ (c,e); ii) PULSE
589 drives expression of LFY-VP16 ($P_{\text{Opto-LFY-VP16-2A-RLuc}}$). Co-expressed RLuc via
590 a self-cleaving 2A peptide serves as proxy of LFY-VP16 expression. LFY-VP16
591 activates expression from the Arabidopsis promoter P_{AtAP1} ($P_{\text{AtAP1-FLuc}}$) (d,f). RLuc
592 and FLuc determinations: $P_{\text{Opto-LFY-VP16-2A-RLuc}}$ (stripped bars) and $P_{\text{AtAP1-FLuc}}$
593 (solid bars) (f). Protoplasts were incubated in darkness, red or blue light, and
594 luminescence determined after 18 h. Data shown are means of FLuc/RLuc of distinct
595 protoplast samples ($n = 4$) (b,e), and RLuc and FLuc means, background values
596 (configuration without $P_{\text{Opto-LFY-VP16-2A-RLuc}}$) subtracted for FLuc ($n = 6$ distinct
597 protoplast samples) (f), SEM. RLU = Relative Luminescence Units.

598 **Fig. 5:** Implementation and characterization of PULSE in *Nicotiana benthamiana*
599 leaves. **(a,b)** Plants *Agrobacterium*-infiltrated with PULSE, P_{Opto}-Venus and a
600 constitutively expressed Cerulean cassette (pROF346) were kept in dark for 2.5 days
601 prior to light treatment for 2 h, 6 h, 9 h (10 $\mu\text{mol m}^{-2} \text{s}^{-1}$ of red light, 10 $\mu\text{mol m}^{-2} \text{s}^{-1}$ of
602 blue light, white light, or darkness). Samples were taken at indicated time points from
603 three different areas of the leaf of two plants for each illumination condition for
604 fluorescence confocal microscopy observation. At least 6 images, with 2 to 8 nuclei
605 per image, were taken for each condition. Representative images are shown (a). The
606 images were used to quantify the ratio of nuclear Venus and Cerulean fluorescence
607 intensities (b). Data is presented as box plot with the median (center line),
608 interquartile range (box) and the minimum to maximum values (whiskers),
609 $12 \leq n \leq 34$ nuclei. The statistical significance is determined by a one way-ANOVA
610 and Dunnett's multiple comparison test. p -values are 0.9696, 0.0001, and 0.0001, for
611 2, 6 and 9 h, respectively for red light treatment; 0.3828, 0.0020, and 0.0071, for 2, 6
612 and 9 h, respectively for white light treatment; 0.0643, 0.0727, 0.9989, for 2, 6 and 9
613 h, respectively for blue light treatment; 0.5051, 0.5251, and 0.7580, for 2, 6 and 9 h,
614 respectively for dark treatment (** $p < 0.01$, *** $p < 0.001$, **** $p \leq 0.0001$, *ns* not
615 significant).

616 **Fig. 6:** *In planta* optogenetic heterologous induction of immunity and conditional
617 subcellular targeting of receptors, and PULSE functionality in Arabidopsis transgenic
618 lines. **(a,b)** PULSE-controlled conditional gain of immunity *in planta*. *N. benthamiana*
619 leaves were *Agrobacterium*-infiltrated with PULSE and P_{Opto}-EFR-GFP. Disks were
620 collected from two different plants and treated with 1 μ M elf18 or mock previous to
621 ROS quantification over time. Luminescence mean values ($n = 8$ leaf disks), SEM.
622 **(c,d)** Conditional targeting of receptors by optogenetically controlled expression of a
623 nanobody (GBP-mCherry) observed by confocal microscopy. *N. benthamiana* leaves
624 were infiltrated with PULSE, P_{Opto}-GBP-mCherry, and P_{CaMV35S}-EFR-GFP constructs 625
(control: without P_{CaMV35S}-EFR-GFP). **(b,d)** Plants were kept in standard growth 626
conditions (16 h white light – 8 h dark) for 2 d prior to induction with 10 μ mol m⁻² s⁻¹
627 red light for additional 16 h (control: white light). **(e)** PULSE functionality in
628 Arabidopsis plants. Seedlings of wild type plants ($n = 6$ seedlings) and two
629 independent Arabidopsis homozygous T3 lines (#4-4, #6-3) transformed with PULSE
630 controlling P_{Opto}-FLuc ($n = 26$ seedlings, each line) were grown for 8 d, subsequently
631 illuminated as indicated and luminescence determined over time. Plotted data are
632 mean values (background values from wild type seedlings subtracted), SEM. RLU =
633 Relative Luminescence Units.

634 **Extended Data Fig. 1.** Model-based functional characterization, and prediction and
635 validation of PULSE function. **(a,b)** Quantitative characterization of On-Off FLuc
636 expression kinetics. Protoplasts of Arabidopsis were transformed with PULSE and
637 first kept in the dark, 12 h for protein (a) and 16 h for mRNA (b) determination
638 assays. Samples were afterwards illuminated with either $10 \mu\text{mol m}^{-2} \text{s}^{-1}$ of red or
639 blue light, or kept in darkness for the indicated time periods. Arrows indicate the time
640 point where the samples were split into different illumination conditions for response
641 and reversibility analyses, e.g. red to dark, red to blue (On-Off), red to blue to red
642 (On-Off-On). Samples were collected every 3 h for 15 h for FLuc and RLuc
643 determinations in a plate reader (a); and at 15 min, 30 min, 1 h, 2 h, 4 h, 4 h 15 min,
644 4 h 30 min, 6 h, 7 h for RT-qPCR determinations of mRNA production (b). The curves
645 are the fits to the ODE-based model. The shaded areas represent the error bands as
646 calculated in 95% confidence intervals with a constant Gaussian error model using
647 the profile likelihood method. Depicted are the FLuc/RLuc ratios for protein
648 expression kinetics of distinct protoplast samples ($n = 6$) (a), and the ratio between
649 starting quantity (SQ) of FLuc and the geometric mean of EF, TIP41L (internal
650 normalization controls) transcripts, of two technical replicates for each transcript (b).
651 **(c)** Model aided prediction of PULSE-controlled protein expression levels as a
652 function of red light intensities and illumination times. The calibrated model yields
653 estimated FLuc/RLuc expression ranges (heatmap). **(d)** Experimental validation of
654 the model predictions of the operating range of PULSE. Selected model simulated
655 expression levels at different red light intensities and illumination times as indicated
656 in (c) were experimentally tested and the resulting FLuc/RLuc ratios ($2 \times \text{SEM}$, $n = 6$
657 distinct protoplast samples) were compared to the predicted values (error bars
658 calculated as in (a,b)). RLU = Relative Luminescence Units.
659

660 **ONLINE METHODS**

661 **Plasmid construction**

662 A description of the plasmid construction can be found in **Supplementary Table 1**.

663 DNA fragments were released by restriction from existing plasmids, amplified by
664 PCR using primers synthesized by Sigma Aldrich or Eurofins genomic (listed in
665 **Supplementary Table 2**), or synthesized by GeneArt, Invitrogen. The PCR reactions
666 were performed using Q5 High-Fidelity DNA Polymerase (New England Biolabs). Gel
667 extractions were performed using NucleoSpin® Gel and PCR Clean-up kit
668 (Macherey-Nagel), or Zymoclean Gel DNA Recovery Kit (Zymo Research).
669 Assemblies were performed using either Gibson⁴³, AQUA⁴⁴, GoldenBraid⁴⁵ or Golden
670 Gate^{46,47} cloning methods prior to transformation into chemically competent

671 *Escherichia coli* strain 10-beta (NEB) or TOP10 (Invitrogen). The plasmid
672 purifications were performed using Wizard® Plus SV Minipreps DNA Purification
673 Systems (Promega), NucleoBond® Xtra Midi kit (Macherey-Nagel) or GeneJET
674 Plasmid Miniprep Kit (Thermo Scientific). All preparations were tested by restriction
675 enzyme digests and sequencing (GATC-biotech/SeqLab). All restriction enzymes
676 were purchased from New England Biolabs or ThermoScientific.

677 **Arabidopsis protoplast isolation and transformation**

678 Protoplasts were isolated from two- to three-week old *Arabidopsis thaliana* plantlet
679 leaves, grown on 12 cm square plates containing SCA medium (0.32 % (w/v)
680 Gamborg B5 basal salt powder with vitamins (bioWORLD), 4 mM MgSO₄·7H₂O, 43.8
681 mM sucrose and 0.8% (w/v) phytoagar in H₂O, pH 5.8, autoclaved, 0.1 % (v/v)
682 Gamborg B5 Vitamin Mix (bioWORLD), in a 23 °C, 16 h light - 8 h dark regime. A
683 floatation method was employed for isolation and the plasmids were transferred by
684 polyethylene glycol-mediated transformation as described before¹⁰. Shortly, plant leaf
685 material was sliced with a scalpel and incubated in dark at 23 °C overnight in MMC

686 solution (10 mM MES, 40 mM $\text{CaCl}_2 \cdot \text{H}_2\text{O}$, mannitol 85 g L^{-1} , pH 5.8, sterile filtered)
687 containing 0.5 % cellulase Onozuka R10 and macerozyme R10 (SERVA
688 Electrophoresis GmbH). After release of the protoplasts with a pipette, the
689 suspension was transferred to a MSC solution (10 mM MES, 0.4 M sucrose, 20 mM
690 $\text{MgCl}_2 \cdot 6\text{H}_2\text{O}$, 85 g L^{-1} mannitol, pH 5.8, sterile filtered) and overlaid with MMM
691 solution (15 mM MgCl_2 , 5 mM MES, 85 g L^{-1} mannitol, pH 5.8, sterile filtered). The
692 protoplasts were collected at the interphase and transferred to a W5 solution (2 mM
693 MES, 154 mM NaCl, 125 mM $\text{CaCl}_2 \cdot 2\text{H}_2\text{O}$, 5 mM KCl, 5 mM glucose, pH 5.8, sterile
694 filtered) prior to counting in a Rosenthal chamber. Mixtures of the different plasmids,
695 as described in the figures, to a final amount of 30-35 μg DNA were used to
696 transform 500,000 protoplasts by dropwise addition of a PEG solution (4 g PEG_{4000} ,
697 2.5 mL of 0.8 M mannitol, 1 mL of 1 M CaCl_2 and 3 mL H_2O). After 8 min incubation,
698 120 μL of MMM and 1,240 μL of PCA (0.32 % (w/v) Gamborg B5 basal salt powder
699 with vitamins (bioWorld)), 2 mM $\text{MgSO}_4 \cdot 7\text{H}_2\text{O}$, 3.4 mM $\text{CaCl}_2 \cdot 2\text{H}_2\text{O}$, 5 mM MES,
700 0.342 mM L-glutamine, 58.4 mM sucrose, 80 g L^{-1} glucose, 8.4 μM Ca-panthotenate,
701 2 % (v/v) biotin from a biotin solution 0.02 % (w/v) 0.1 % (v/v) in H_2O , pH 5.8, sterile
702 filtered, 0.1 % (v/v) Gamborg B5 Vitamin Mix, 64.52 μg μL^{-1} ampicillin) were added to
703 get a final volume of 1.6 mL of protoplast suspension.

704 After transformation, protoplasts were then divided in different 24-well plates in 960
705 μL aliquots (300,000 protoplasts-necessary to measure six technical replicates for
706 both FLuc and RLuc) or in 640 μL aliquots (200,000 protoplasts-necessary to
707 measure 4 technical replicates for both FLuc and RLuc). Afterwards, the plates were
708 either illuminated with LED arrays with the appropriate wavelength and intensity (as
709 indicated in the figures) for 18 - 20 h at 19 - 23 $^\circ\text{C}$ unless indicated otherwise.

710 **Illumination conditions**

711 Custom made LED light boxes were used as described before^{10,48}. The panels
712 contain LEDs from Roithner: blue (461 nm), red (655 nm), far-red (740 nm) and white
713 LEDs (4000K). For blue, red or far-red light treatment, the intensity was adjusted to
714 $10 \mu\text{mol m}^{-2} \text{s}^{-1}$ unless indicated otherwise. White LEDs were supplemented with blue
715 and far-red LEDs in order to have an equivalent ratio of blue, red and far-red light
716 similar to the sunlight spectra (simulated white light). The intensity of the white light
717 LED was adjusted to $10 \mu\text{mol m}^{-2} \text{s}^{-1}$ for the following wavelength ranges: blue 420 -
718 490 nm, red 620 - 680 nm, and far-red 700 - 750 nm⁴⁹ (see spectra shown in
719 **Supplementary Fig. 7**). For the *Nicotiana benthamiana* GUS experiment the plants
720 were kept, prior light treatment, in the plant incubator with fluorescent tubes (cool
721 daylight, OSRAM). Cell- and plant- handling and sampling was done, when needed,
722 under green LED (510 nm) light which does not affect the PULSE system. Spectra
723 and intensities were obtained with a spectroradiometer (AvaSpec-ULS2048 with
724 fiber-optic FC-UVIR200-2, AVANTES).

725 **Luciferase protoplasts assay**

726 Firefly (FLuc) and Renilla luciferase (RLuc) activities were quantified in intact
727 protoplasts as detailed elsewhere¹⁰. Six technical replicates of 80 μL protoplast
728 suspensions (approximately 25,000 protoplasts) were pipetted into two separate 96-
729 well white flat-bottom plates (Costar) for simultaneous parallel quantification of both
730 luciferases. Addition of 20 μL of either FLuc substrate (0.47 mM D-luciferin (Biosynth
731 AG), 20 mM tricine, 2.67 mM $\text{MgSO}_4 \cdot 7\text{H}_2\text{O}$, 0.1 mM $\text{EDTA} \cdot 2\text{H}_2\text{O}$, 33.3 mM
732 dithiothreitol, 0.52 mM adenosine 5'-triphosphate, 0.27 mM acetyl-coenzyme A, 5
733 mM NaOH, 264 μM $\text{MgCO}_3 \cdot 5\text{H}_2\text{O}$, in H_2O , pH 8), or RLuc substrate (0.472 mM
734 coelenterazine stock solution in methanol, diluted directly before use, 1:15 in
735 phosphate buffered saline, PBS) was performed prior luminescence determination in
736 a plate reader (determination of 20 min kinetics, integration time 0.1 s). RLuc

737 luminescence was measured with a BertholdTriStar2 S LB 942 multimode plate
738 reader and FLuc luminescence was determined with a Berthold Centro XS3 LB 960
739 microplate luminometer. When applicable, FLuc/RLuc was determined and the
740 average of the replicates and SEM was plotted ($n = 4 - 6$).

741 **RNA isolation and quantitative RT-qPCR**

742 Protoplasts were isolated and transformed as described before. The protoplasts were
743 kept in the dark, at room temperature for 16 h prior illumination treatment. At the
744 indicated time point and illumination condition, samples containing *ca.* 10^6
745 protoplasts were collected by centrifugation (10 min, 100 *g*) and were frozen in liquid
746 N_2 for posterior RNA extraction. The RNA was extracted with a PeqGold Plant RNA
747 kit following the user specifications. The samples were treated with DNase I (Thermo
748 Scientific). The cDNA was synthesized from 500 ng of the RNA samples, using the
749 Revert Aid Reverse Transcriptase (Thermo Scientific) and diluted 1:100 prior to
750 qPCR. Expression levels on the samples were measured in duplicates using SYBR®
751 Green Master Mix (Bio-Rad) with specific primer pairs in a Real-time PCR cycler
752 CFX96 (Bio-Rad) as described before⁵⁰. A DNA mass standard for each gene was
753 prepared in serial dilutions of 10^2 to 10^7 copies and measured in parallel with the
754 samples. The genes TIP41-like family protein, TIP41L (*At4g34270*), and Elongation
755 Factor, EF (*At5g19510*), were used as an internal reference genes. Starting quantity
756 values of the samples were calculated using the mass standard curve and
757 normalized with the internal reference gene. Primer pairs used to amplify the DNA
758 mass standard are oROF422/oROF423 for FLuc, oROF518/oROF519 for TIP41L,
759 and EF STD 5'/3'⁵⁰ for EF. Specific primer pairs used for the qPCR are
760 oROF424/oROF425 for FLuc cDNA, oROF514/oROF515 for TIP41L cDNA, and EFc
761 RT 5'/3'⁵⁰ for EF cDNA (**Supplementary Table 2**).

762 ***Agrobacterium tumefaciens* transformation**

763 Electro-competent *Agrobacterium tumefaciens* strains C58 (pM90), GV3101 (pM90),
764 containing pSOUP helper plasmid, or AGL1 was transformed with the plasmid of
765 interest. Clones growing in YEP media (10 g L⁻¹ yeast extract, 10 g L⁻¹ bacto
766 peptone, 5 g L⁻¹ NaCl, pH 7.0) supplemented with appropriate antibiotics were
767 selected and each transcriptional unit was confirmed by colony PCR using Q5 DNA
768 polymerase (New England Biolabs).

769 **Transient transformation of *Nicotiana benthamiana* plants**

770 *A. tumefaciens* cultures were adjusted to OD_{600nm} = 0.1 - 0.2 in infiltration medium
771 (10 mM MgCl₂, 10 mM MES, 200 μM acetosyringone, in H₂O, pH 5.6). The cultures
772 were mixed in a volume ratio 1:1 with an *A. tumefaciens* culture coding for the RNA
773 silencing suppressor p19. The cultures were incubated for 3 h at room temperature in
774 the dark prior infiltration through the adaxial part of leaves from 4- to 5-week old *N.*
775 *benthamiana* grown in the greenhouse as described before⁵¹. The plants were
776 incubated for 2-3 days in the indicated illumination conditions prior to light treatment
777 and analysis by microscopy or enzymatic GUS reporter assay.

778 **GUS reporter assay in *Nicotiana benthamiana* leaves**

779 After the illumination of the plants as depicted in the **Supplementary Fig. 5**, two
780 disks of 0.8 cm diameter from different leaves for each illumination treatment were
781 cut and incubated on GUS substrate (100 mM Na₂HPO₄, 100 mM NaH₂PO₄, 782
adjusted to pH 7.0, 2 mM K₃Fe(CN)₆, 2 mM K₄Fe(CN)₆, 2 mM X-Gluc, 0.20 % Triton 783 X-
100, in H₂O) for 3 h at 37°C in dark⁵². The stained disks were washed several
784 times with 70% ethanol to remove the chlorophylls and the pictures were taken with a
785 Nikon D3200 camera.

786 **Confocal imaging of *Nicotiana benthamiana* leaf material**

787 For the experiments of optogenetically controlled Venus, leaves of one to two plants
788 for each condition were transiently transformed and incubated for 2.5 days in the

789 dark, and afterwards illuminated for 2 h, 6 h or 9 h with the appropriate wavelength
790 as indicated in **Fig. 5a,b**. Samples were taken at indicated time points from three
791 different areas of the leaves of the two plants and imaged with a LSM 780 Zeiss laser
792 scanning confocal microscope. The constitutive Cerulean was excited with a Diode
793 405-30 at 405 nm. The optogenetically controlled Venus expression was excited with
794 an Argon laser at 514 nm. The emission was detected at 440-500 nm for Cerulean
795 and 516-560 nm for Venus. For each condition at least 6 images, with 2 to 8 nuclei
796 per image, were generated. The fluorescence intensities of nuclei were quantified
797 using ImageJ. For each nucleus, an area was selected by using the elliptical
798 selection tool and the mean grey values of the Cerulean and Venus channels were
799 measured, respectively. The ratio of Venus and Cerulean was calculated and
800 expressed in percentage, and plotted for 12 - 34 nuclei (see Life Science reporting
801 summary for detailed information).

802 For the experiments of conditional targeting and immunity control, *N. benthamiana*
803 were grown for 2 d in 16 h simulated white light – 8 h dark cycle (see
804 **Supplementary Fig. 7**), hereafter half of the plants were grown for 16 h in red light
805 only to induce expression (red light-induced), the other half were grown in simulated
806 white light for 16 h (white light control). The white light control plants were further
807 grown for 16 h after the experiments in red light to induce expression as control for
808 successful transformation. Samples were taken for confocal observation. Confocal
809 laser scanning microscopy was performed with a Leica SP8 confocal microscope
810 using a 20x/0.75 HC PL APO CS IMM CORR lens with a scanning speed of 200 Hz.
811 EFR-GFP and GBP-mCherry were excited with a white light laser at 488 nm and 561
812 nm, respectively. The emission was detected at 500 - 550 nm for GFP and 575 - 630
813 nm for mCherry.

814 **Reactive oxygen species (ROS) burst assay**

815 Samples were collected from *N. benthamiana* leaves transformed with the indicated
816 constructs or only infiltration buffer (two plants were used for each illumination
817 treatment). ROS production was determined using a BMG CLARIOstar plate reader
818 and following the protocol by Trujillo⁵³ for Arabidopsis leaves with the following
819 modifications: samples were prepared with a 4 mm biopsy puncher and placed in 150
820 μ L sterile tap water for 3 h in dark to get rid of any ROS production originating from
821 the sample harvest before elf18 or control treatment. Approximately 20 min before
822 addition of 1 μ M elf18, water was removed from leaf samples and replaced with
823 reaction solution⁵³, incubated for ca. 3 min before background measurement of ROS
824 production was performed for ca. 15 min followed by addition of reaction solution with
825 elf18 or without (mock control).

826 **Stable transformation of *Arabidopsis thaliana***

827 Four to five week old *A. thaliana* ecotype Columbia plants grown in a plant chamber
828 (16 h light – 8 h dark, 22°C) were transformed via *Agrobacterium tumefaciens* by
829 floral dip as described earlier⁵⁴ with minor modifications. *Agrobacterium* cells

830 transformed with the corresponding constructs (described in **Supplementary Table**
831 **1**) were grown to OD_{600nm} values between 0.6 and 0.9, centrifuged and gently
832 resuspended in 2.4 g/L Murashige & Skoog medium including vitamins (Duchefa
833 Biochemie), 5% (w/v) sucrose, 0.05% (v/v) Silwet L-77 (bioWORLD) and 222 nM 6-
834 Benzylaminopurine (Duchefa Biochemie).

835 Transformants were selected by seeding in SCA plates (0.32 % (w/v) Gamborg B5
836 basal salt powder with vitamins (bioWORLD), 4 mM MgSO₄·7H₂O, 43.8 mM sucrose,
837 0.8 % (w/v) phytoagar, 0.1 % (v/v) Gamborg B5 Vit Mix (bioWORLD), pH 5.8)
838 containing 30 μ g mL⁻¹ kanamycin (Duchefa Biochemie) and 150 μ g mL⁻¹ ticarcillin
839 disodium/potassium clavulanate (Duchefa Biochemie). The positive T1 plants were

840 checked for expression of the reporter/normalization gene when possible, and the T2
841 seeds were collected and selected in kanamycin containing media. The lines
842 exhibiting a segregation ratio 3:1 (resistant to sensitive) were propagated until a T3
843 generation and homozygous lines were selected and used for further experiments.
844 The transgenic PULSE lines are functional and viable.

845 **Luciferase assay in *Arabidopsis thaliana* plants**

846 Seeds from the *A. thaliana* lines ($n = 26$ for the PULSE lines, $n = 6$ for the wild type
847 controls) were seeded in individual wells of white 96-well white flat-bottom plates
848 (Costar), containing 200 μL of 2.4 g L^{-1} Murashige & Skoog medium including
849 vitamins (M0222, Duchefa Biochemie) and 0.8 % (w/v) phytoagar (bioWORLD).
850 They were kept for 3 - 4 days at 4°C in the dark, and illuminated for 1 h with
851 simulated white light (see spectra in **Supplementary Fig. 7**) on the fourth day. Then
852 the plate was placed in simulated white light with photoperiod (16 h light – 8 h dark)
853 for 4 days. Addition of 20 μL of FLuc substrate 1.667 mM D-luciferin (from a 20 mM
854 stock in DMSO, Biosynth AG) and 0.01 % Triton in H_2O was performed on the fourth
855 day prior starting the measurements. The plate was sealed with an optically clear film
856 (Sarstedt) thinly perforated. Luminescence was measured, 1 - 2 days after addition of
857 the substrate, in a Berthold Centro XS3 LB 960 microplate reader every hour during
858 several days (1 min delay, 0.5 integration time) while being illuminated as indicated.
859 The background readout levels of *Arabidopsis* wildtype seedlings were averaged,
860 and the value was subtracted from the rest of the lines for each time point.

861 **Sample size, replication and statistics**

862 Data shown in the figures are representative experiments from at least two
863 independent experiments (see Life Science Reporting Summary for detailed
864 information). The sample number per experiment is indicated in each corresponding

865 figure. Plotting and statistical tests were performed with GraphPad or MATLAB
866 software.

867 **DATA AND MATERIAL AVAILABILITY STATEMENT**

868 Source data for the figures are available (Source Data .xls files). The raw and
869 associated data that support the findings of this study, and biological material and
870 plasmid maps are available from the corresponding author upon request.

871 **CODE AVAILABILITY STATEMENT**

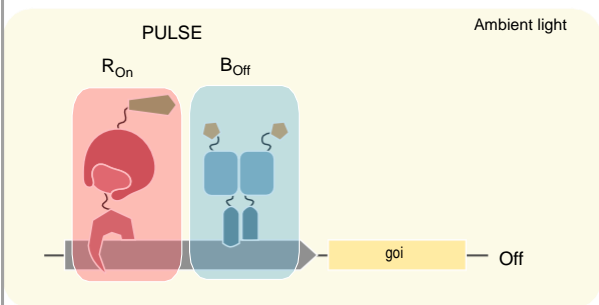
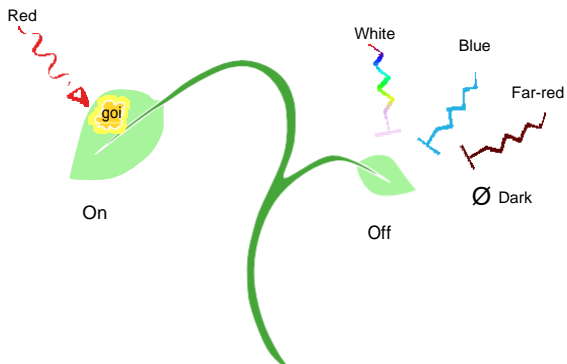
872 The numerical integration, fitting process and identifiability analysis with the profile
873 likelihood method were performed in MATLAB using the freely available
874 Data2Dynamics software. Details relative to the equations used can be found in the
875 **Supplementary Information.**

876

877 **METHODS-ONLY REFERENCES**

- 878 43. Gibson, D. G. *et al.* Enzymatic assembly of DNA molecules up to several hundred
879 kilobases. *Nat. Methods* **6**, 343 (2009).
- 880 44. Beyer, H. M. *et al.* AQUA Cloning: A Versatile and Simple Enzyme-Free Cloning
881 Approach. *PLoS ONE* **10**, e0137652 (2015).
- 882 45. Sarrion-Perdigones, A. *et al.* GoldenBraid 2.0: A Comprehensive DNA Assembly
883 Framework for Plant Synthetic Biology. *Plant Physiol.* **162**, 1618 (2013).
- 884 46. Binder, A. *et al.* A Modular Plasmid Assembly Kit for Multigene Expression, Gene
885 Silencing and Silencing Rescue in Plants. *PLoS ONE* **9**, e88218 (2014).
- 886 47. Weber, E., Engler, C., Gruetzner, R., Werner, S. & Marillonnet, S. A Modular
887 Cloning System for Standardized Assembly of Multigene Constructs. *PLoS ONE*
888 **6**, e16765 (2011).

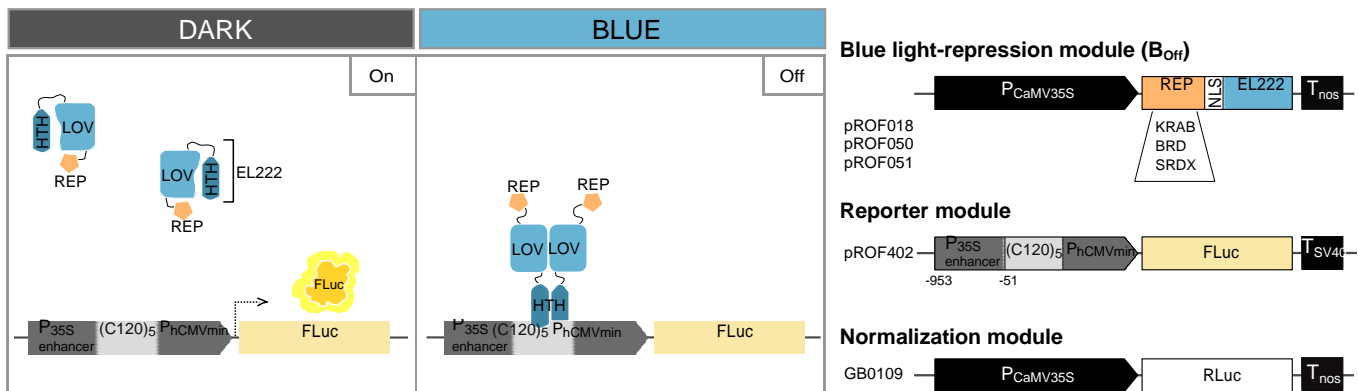
- 889 48. Müller, K., Zurbriggen, M. D. & Weber, W. Control of gene expression using a
890 red- and far-red light-responsive bi-stable toggle switch. *Nat. Protoc.* **9**, 622
891 (2014).
- 892 49. Sellaro, R. *et al.* Cryptochrome as a Sensor of the Blue/Green Ratio of Natural
893 Radiation in Arabidopsis. *Plant Physiol.* **154**, 401 (2010).
- 894 50. Bauer, P. Regulation of iron acquisition responses in plant roots by a transcription
895 factor: Regulation of Iron Acquisition Responses. *Biochem. Mol. Biol. Educ.* **44**,
896 438–449 (2016).
- 897 51. Vazquez-Vilar, M. *et al.* GB3.0: a platform for plant bio-design that connects
898 functional DNA elements with associated biological data. *Nucleic Acids Res.* **45**,
899 2196–2209 (2017).
- 900 52. Naranjo-Arcos, M. A. *et al.* Dissection of iron signaling and iron accumulation by
901 overexpression of subgroup Ib bHLH039 protein. *Sci. Rep.* **7**, 10911 (2017).
- 902 53. Trujillo, M. Analysis of the Immunity-Related Oxidative Bursts by a Luminol-Based
903 Assay. in *Environmental Responses in Plants: Methods and Protocols* (ed.
904 Duque, P.) 323–329 (Springer New York, 2016). doi:10.1007/978-1-4939-3356-
905 3_26.
- 906 54. Clough, S. J. & Bent, A. F. Floral dip: A simplified method for *Agrobacterium*-
907 mediated transformation of *Arabidopsis thaliana*. *Plant J.* **16**, 735–743 (1998).



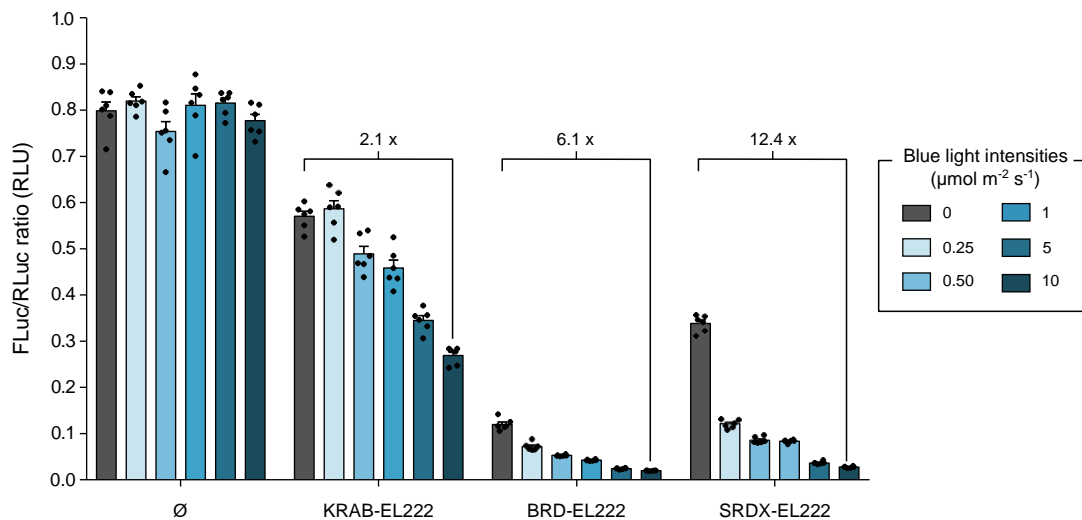
	Wavelength composition of light			Gene expression
	Blue	Red	Far-red	
W	+	+	+	-
B	+	-	-	-
R	-	+	-	+
FR	-	-	+	-
D	-	-	-	-

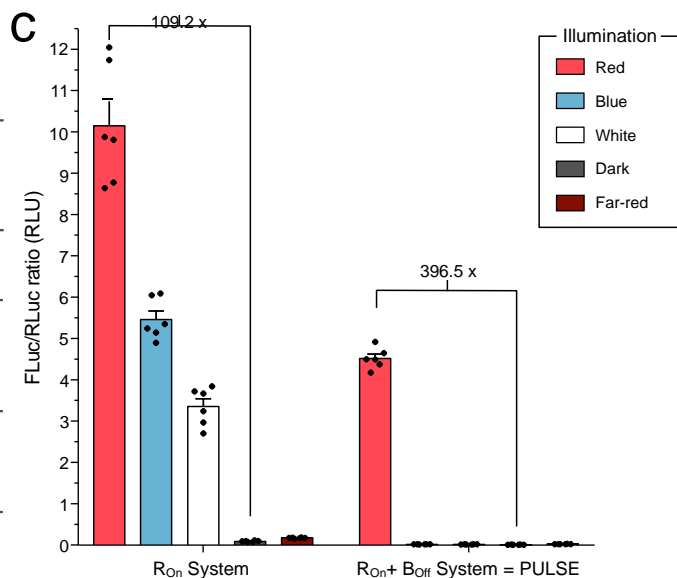
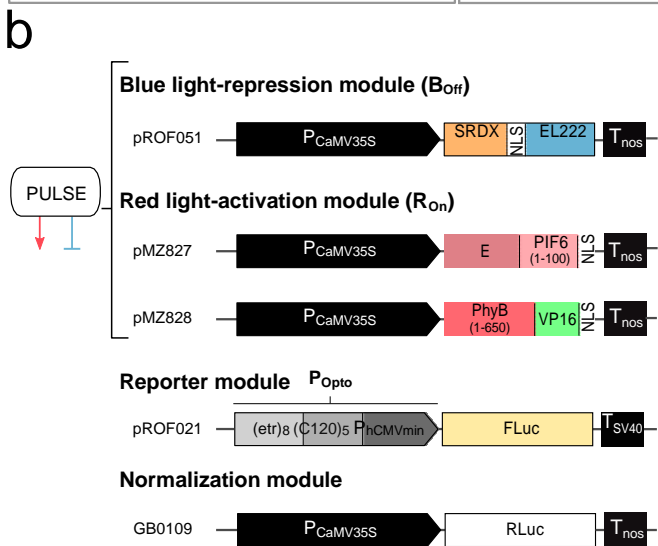
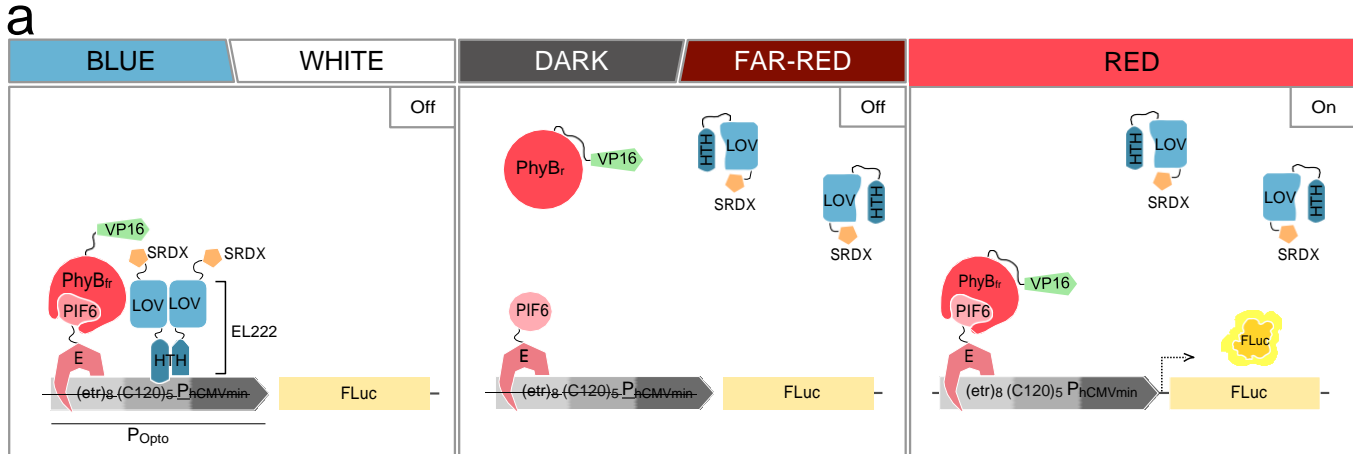
Illumination conditions

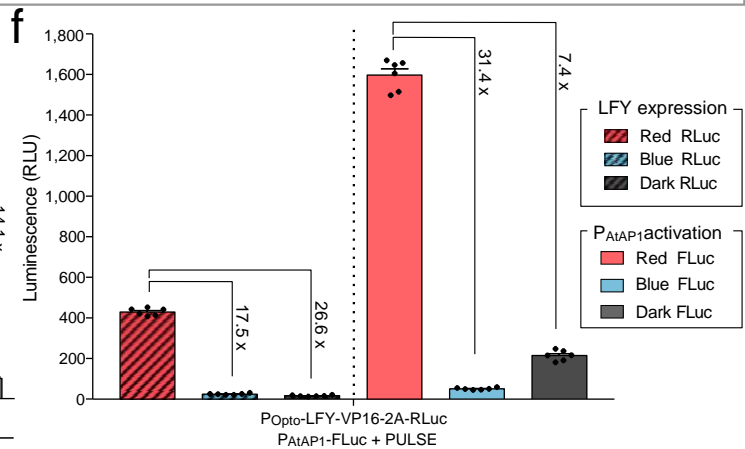
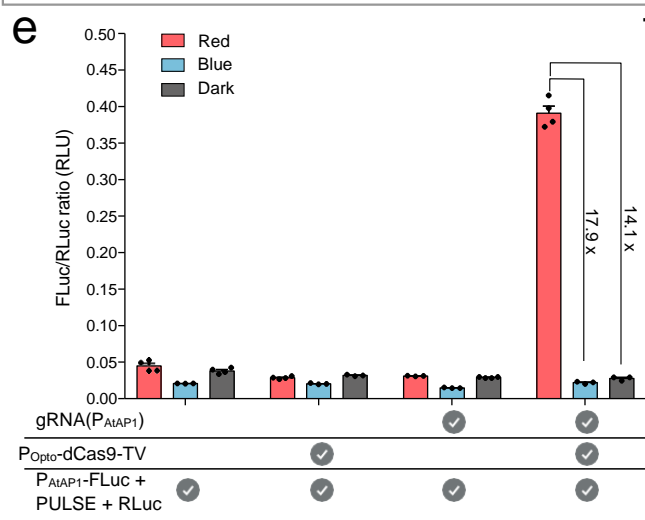
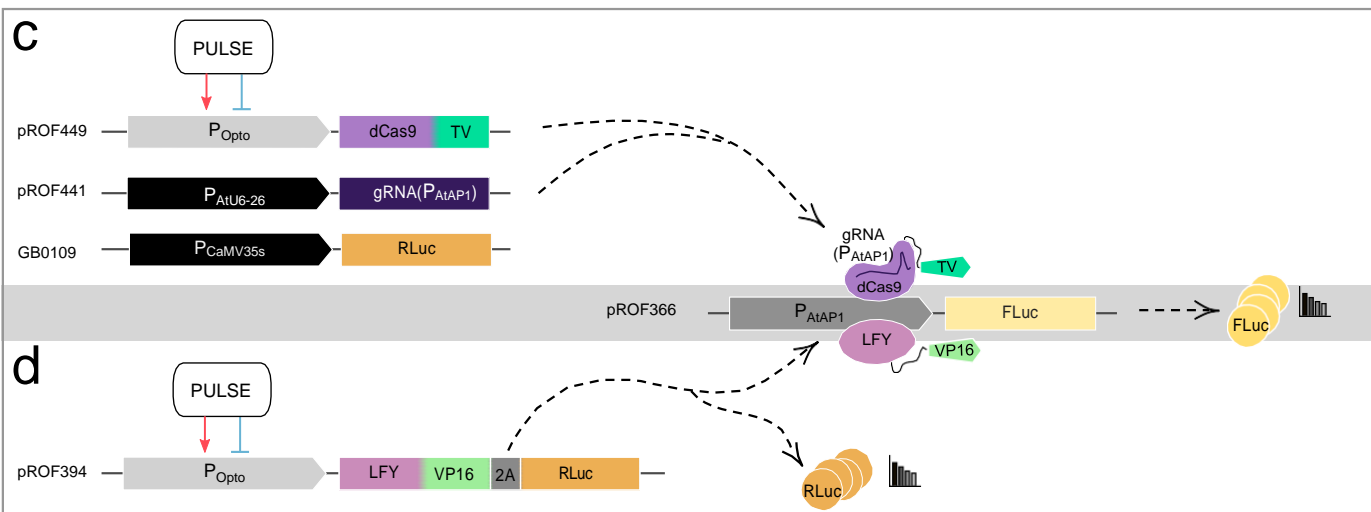
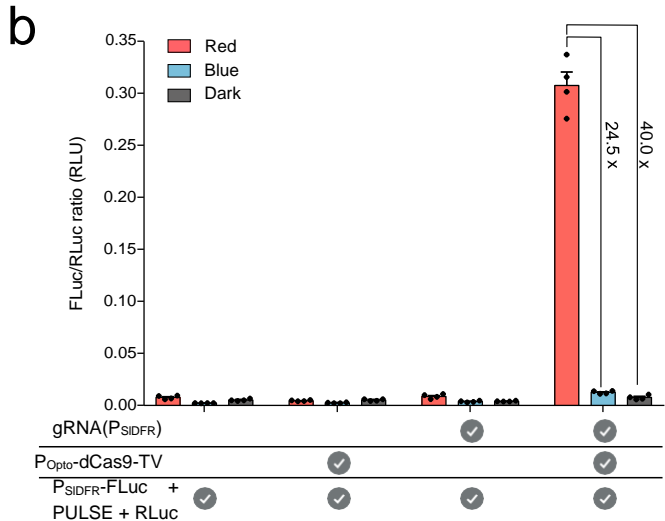
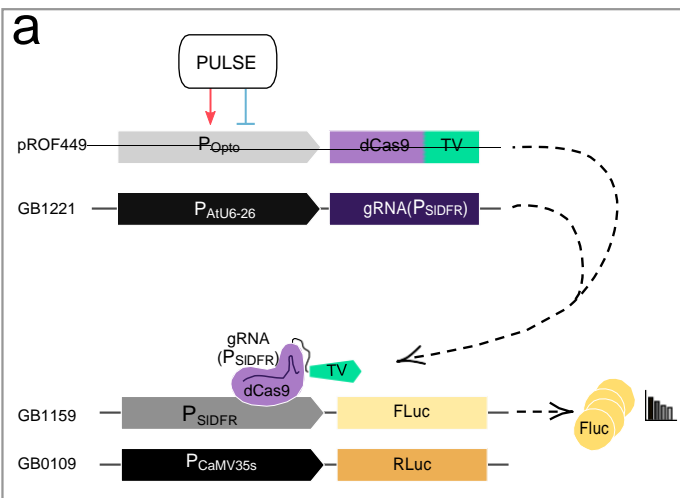
a

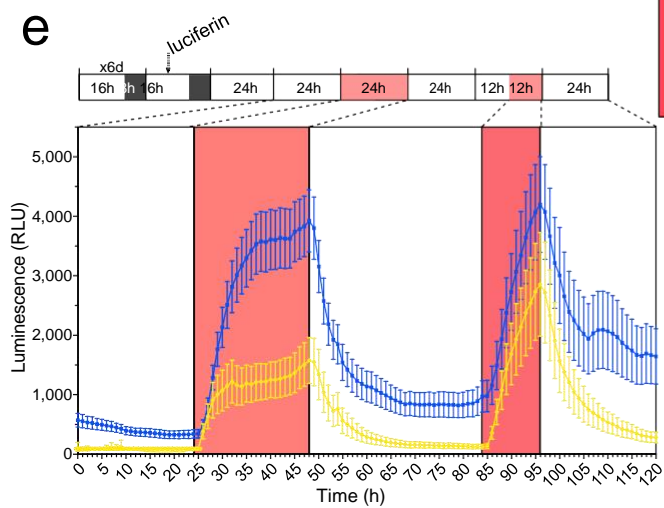
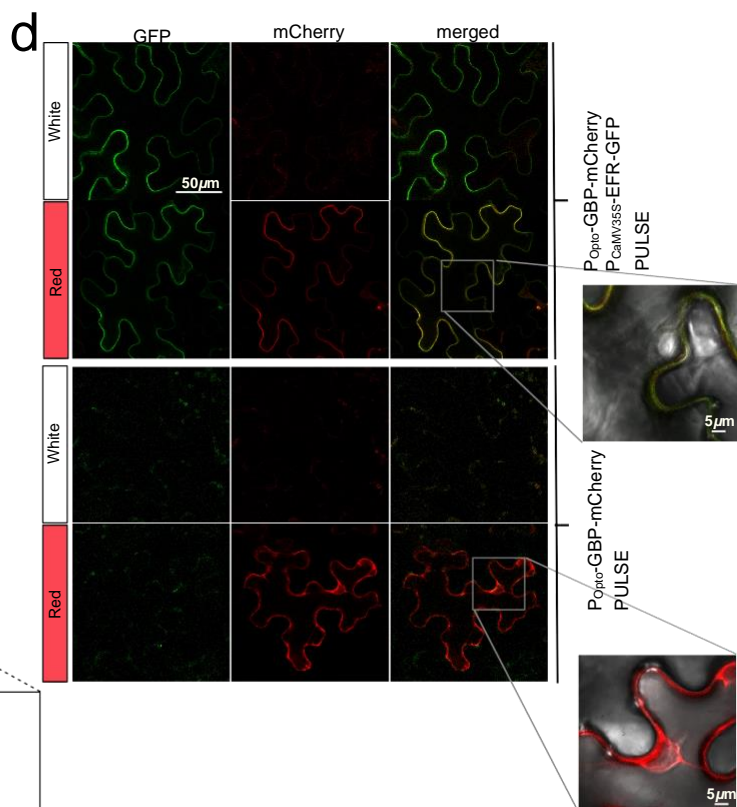
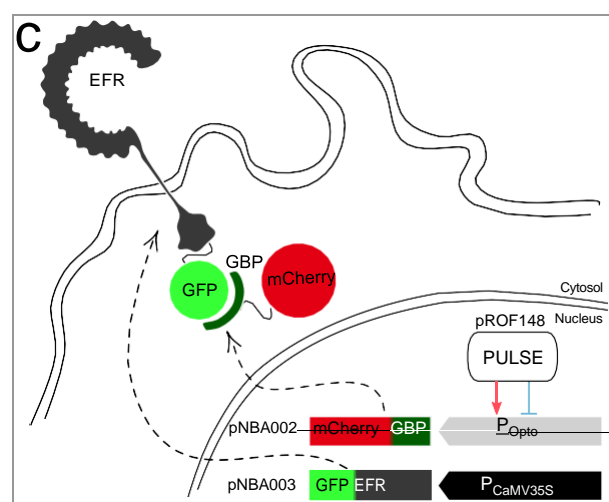
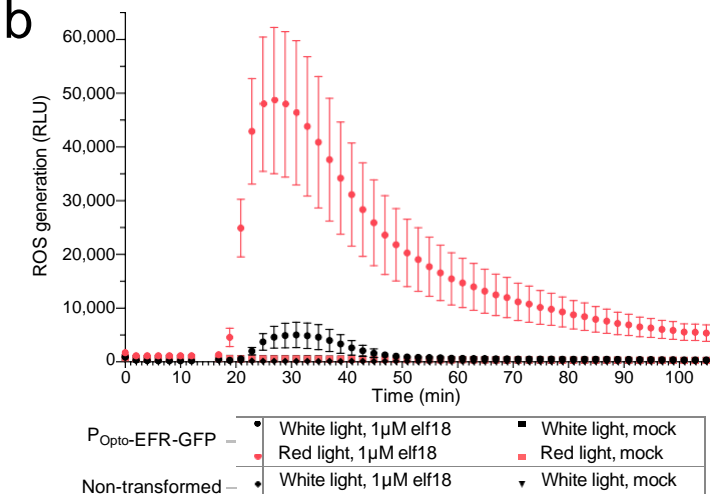
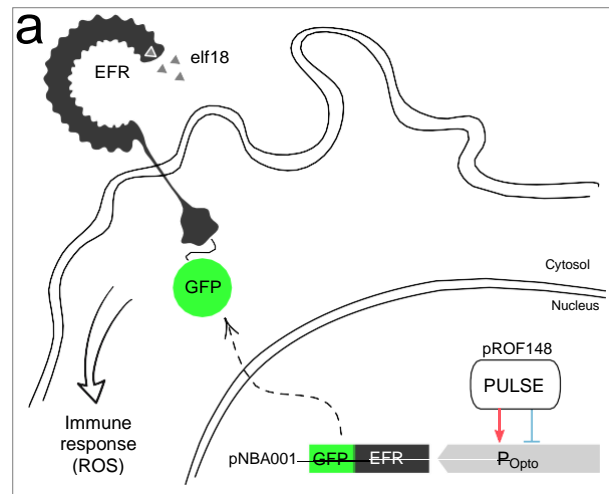


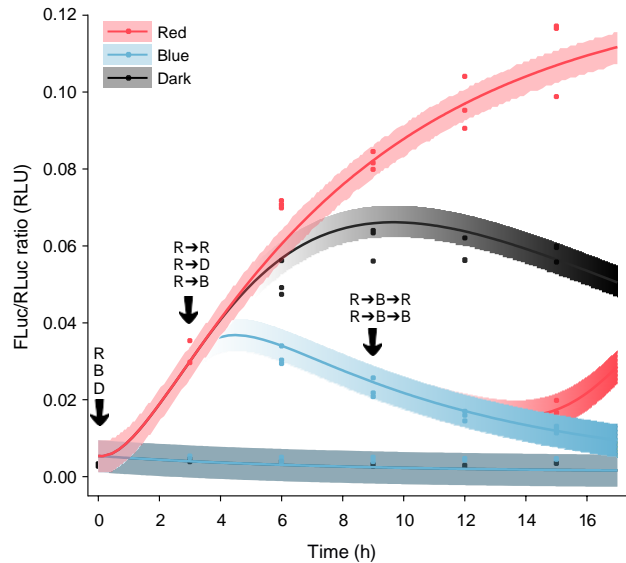
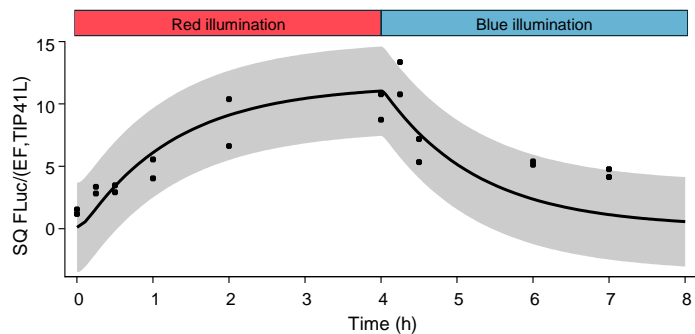
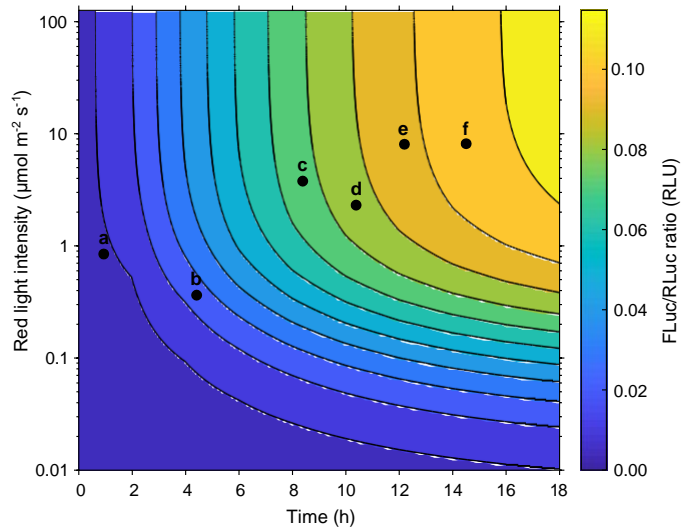
b









a**b****c****d**